Estimation of CFC-11 emissions from coal combustion in China

Zhenzhen Niu [1], Shaofei Kong [1, 2 *], Qin Yan [1], Yi Cheng [1], Huang Zheng [1], Yao Hu [1], Jian Wu [1, 2], Xujing Qin [1], Haoyu Dong [1], Weisi Jiang [1], Yingying Yan [1], Wei Liu [3], Feng Ding [3], Yongqing Bai [4], Shihua Qi [1, 2]

[1] Department of Atmospheric Sciences, School of Environmental Studies, China University of Geosciences (Wuhan), Wuhan, 430078, China

[2] Research Centre for Complex Air Pollution of Hubei Province, Wuhan, 430078, China

[3] Hubei Province Academy of Eco-Environmental Sciences, Wuhan, 430072, China

[4] Institute of Heavy Rain, China Meteorological Administration, Wuhan, 430205, China

* *Corresponding to Shaofei Kong (kongshaofei@cug.edu.cn)*

Abstract

The trichlorofluoromethane (CFC-11) emission from its production and use (PAU) has drawn wide attention, while its combustion sources have been overlooked. This study identified CFC-11 emission factors (EFs) as 3.6, 3.2, and 0.025 mg kg^{-1} from the combustion of domestic chunk coal, honeycomb briquette, and coal-fired power plant, respectively. A multi-year (2000~2021) emission inventory of CFC-11 from coal combustion was established in China. Results indicated that the CFC-11 annual emission from coal combustion in China was averaged as 233.5 t yr^{-1}. It exhibited fluctuations and held an overall upward trend, increasing from accounting for 0.8% of PAU emissions in 2000 to 9.8% in 2021, with the peak value appearing in 2016. In Shandong and Hebei provinces with high coal consumption amounts, the CFC-11 emissions from coal combustion increased by approximately 74% during 2014~2017 compared to 2011~2012. At the Gosan station close to Chinese mainland, CFC-11 emitted from coal combustion in Hebei and Shandong was approximately occupied by ~30% of its average concentration during January 2016. An additional climate effect of the clean heating and coal-to-electricity policies in China was also observed, with an obvious decrease (2.2×10^6 t and 3.4×10^7 t) of CO_2-equivalent emission. This study provides substantial evidence of CFC-11 emission from coal combustion and highlights the role of combustion emission under the background of reducing CFC-11 from PAU. The data compiled in this work can found at https://doi.org/10.6084/m9.figshare.28523063 (Niu et al., 2025).

Keywords: Coal combustion; Trichlorofluoromethane emissions; Emission inventory; Global warming potential; WRF-FLEXPART simulation

1. Introduction

Trichlorofluoromethane (CFC-11) has been widely used as a blowing agent for foams incorporated into buildings and consumer products since the 1950s (McCulloch et al., 2001; Rigby et al., 2019). The lifetime of CFC-11 exceeds 50 years, allowing it to accumulate in the atmosphere (Guo et al., 2009; Lickley et al., 2021; Rigby et al., 2013). CFC-11 could deplete stratospheric ozone through photodissociation (Fleming et al., 2020; Molina & Rowland, 1974), and served as a reference compound for calculating ozone depletion potential (ODP) (Western et al., 2023). Over a 100-year time horizon, CFC-11 has a global warming potential (GWP) thousands of times greater than that of carbon dioxide (CO_2) (Chiodo & Polvani, 2022; Polvani et al., 2020), the GWP values of CFC-11 and CO_2 were 7090 and 1, respectively (Burkholder et al., 2022). An accurate understanding of CFC-11 emissions was helpful for assessing the impact of China's implementation of the Montreal Protocol (Fang et al., 2018).

The production and consumption of CFC-11 for emissive applications were phased out globally in 2010 according to the Montreal Protocol released in 1987 (Park et al., 2021). It results in a declining trend of its global atmospheric concentration (Park et al., 2021), and an expectation for ozone-layer recovery throughout the 21st century (Scientific assessment of ozone depletion, 2019). However, since 2012, the decline rate of atmospheric CFC-11 emission has significantly slowed by about 50% (Montzka et al., 2018). Eastern China has been identified as a hotspot for unexpected increased emissions of CFC-11 (Park et al., 2021). Former studies attributed it to new productions of CFC-11 in Eastern China (Montzka et al., 2018; Rigby et al., 2019), especially for blowing closed-cell insulating foam (McCulloch et al., 2001). Based on ambient monitoring data, former studies simulated CFC-11 emissions increased by 29.4% globally (Montzka et al., 2021), 58.3% in East Asia (Adcock et al., 2020), and 130.7% in eastern China (Park et al., 2021) during 2014~2017 compared to corresponding values of 2011~2012. They concluded that the annual emissions from

existing CFC-11 banks alone could not fully explain the observed increase, highlighting a need to evaluate other potential sources for unexpected emissions (Montzka et al., 2018). Therefore, the identification of new CFC-11 emission sources and updating its emission estimation are urgent works.

There are two popular methods frequently adopted to estimate CFC-11 emissions. The first was estimating its emissions based on atmospheric observation dataset, including the inverse modeling approach which identified the CFC-11 emission using two backward-running Lagrangian models, the UK Met Office Numerical Atmospheric-dispersion Modelling Environment (NAME) and the FLEXible PARTicle dispersion model (FLEXPART) (Park et al., 2021), and ratio method which according to a correlation of CFC-11 with tracers holding clear emissions (Zhang et al., 2014). Many tracers were adopted in former studies, such as carbon monoxide (CO), chloroform ($CHCl_3$), and carbon tetrachloride (CCl_4) (Adcock et al., 2020; Huang et al., 2021). CO was widely selected as its emission inventory was established well and updated frequently by MEIC (Multiresolution Emission Inventory for China, http://meicmodel.org.cn/#firstPage). The essential precondition is that the CFC-11 and CO sources were co-located (Dhomse et al., 2019; Huang et al., 2021; Kim et al., 2010). However, CO is a tracer for incomplete combustion (Zeng et al., 2020). If the CFC-11 emission amounts were obtained by multiplying CO emission amounts with a CFC-11/CO ratio from a linear fit, the results were untenable for the following two reasons: (1) CFC-11/CO ratios selected varied in different researches, as 0.087 (Huang et al., 2021), 0.079 (Huang et al., 2021), 0.027~0.069 (Palmer et al., 2003), and 0.022 (Shao et al., 2011). There was no objective criterion for selecting the CFC-11/CO ratios. (2) The hypothetical co-locations of CFC-11 and CO do not mean that their sources are the same. The obtained CFC-11 emission amounts through this method actually mean that CFC-11 is only related to combustion sources.

The second method to estimate CFC-11 emissions was a bottom-up method. The CFC-11 emission inventory was estimated based on the reported CFC-11 production

and use (PAU) amounts from different sectors, including foam blowing, solvents, and refrigerators (Fang et al., 2018; Wan et al., 2009; Zhao et al., 2011), and combustion sources (like coal combustion, diesel combustion, etc.) were always not included. Additionally, in the fields of source profiles of volatile organic compounds (VOCs), CFC-11 has been frequently detected for various types of combustion sources (Gong et al., 2019; SPECIATE Version 5.3; Sha et al., 2021; Sun et al., 2019) The emitted mass concentrations or emission factors of CFC-11 from various combustion sources have also widely reported, such as power plant (12.5 μg m^{-3}) (Shi et al., 2015), gasoline and diesel vehicles (0.01~0.06 mg km^{-1}) (Wang et al., 2020), and coal combustion (0.07~0.51 ppbv) (Li et al., 2003). CFC-11 can be formed by the combustion of coal that contains the necessary elements of carbon, chlorine, and fluorine (Jin et al., 2025; Luo et al., 2004). The level of CFC-11 has been detected at ppb levels in combustion (Pons et al., 2019), which is 3 magnitudes higher than its ambient levels. To the best of our knowledge, the emission inventory of CFC-11 emissions from combustion sources has not been reported.

To sum up, we detected the emission factors (EFs) of CFC-11 from domestic coal combustion (chunk coal and honeycomb briquette) and coal-fired power plants with a unified dilution sampling method. An emission inventory with high spatial resolution of CFC-11 from coal combustion in China during 2000~2021 was first established. The variation trends of CFC-11 emitted from coal combustion and PAU were compared. The impact of CFC-11 emissions from coal combustion in the hotspots of Shandong and Hebei provinces on coastal air was simulated with the WRF-FLEXPART model. This study provides a quantitative assessment of CFC-11 emissions from coal combustion in China, which will provide new insights for identifying its variation trend in ambient air and refining the projection of stratospheric ozone layer recovery.

2. Methods

2.1 Source sampling

To ensure the representativeness and applicability of the emission factors, the combustion experiments were designed to closely simulate real-world domestic coal combustion conditions in rural China. A total of 10 kinds of chunk coals and 11 kinds of honeycomb briquettes were collected and burned in the laboratory in Wuhan. The annual average ambient level of CFC-11 was 0.6 μg m^{-3} in the year 2023. Fuels were collected from eight agricultural regions of China (Figure S1), including the Northeast Plain (Heilongjiang, Jilin, and Liaoning), Arid and semi-arid regions of north China (Inner Mongolia, Ningxia, Gansu, and Xinjiang), Loess Plateau (Shaanxi and Shanxi), North China plain (Anhui, Beijing, Hebei, Henan, Jiangsu, Shandong, Shanghai and Tianjin), Yangtze Plain (Hubei, Hunan, Jiangxi, and Zhejiang), Sichuan Basin (Sichuan and Chongqing), Yunnan-Guizhou Plateau (Guangxi, Guizhou, and Yunnan), Tibet Plateau (Qinghai and Xizang) and South China (Fujian, Guangdong, and Hainan). The specific information on fuel collection can be seen in Table S1. If the fuel in one region had not been collected, the fuel emission characteristics of the neighboring provinces were used as a substitute.

To minimize the impact of ignition smoke, both honeycomb briquettes and chunk coal were lit from beneath pre-measured charcoal. An electric oven was used to ignite the charcoal, allowing it to burn until visible smoke dissipated. The combustion state was controlled by adjusting the stove's bottom air door: fully open for flaming and closed for smoldering. This method replicated the actual burning practices observed in rural China (Yan et al., 2020; Yan et al., 2022). For each test, about 0.8 kg chunk coals and 1.5 kg honeycomb briquettes (three pieces) were burned. The stove used was a typical household furnace purchased from a local market, with an outer diameter, inner diameter, and height of 30, 12, and 43 cm, respectively. An electronic scale was positioned at the bottom of the stove to record the variation of fuel quality. Flue gases were drawn with a sampling gun (1.5 m higher than the flame) and then diluted ~30

150 times with a dilution system (TH-150, Wuhan Tianhong Ltd., China). The equipment
151 settings can be referred to our previous studies (Yan et al., 2020, 2022). The diluted
152 gases were collected into a 4 L Tedlar bag at a flow rate of 150 mL min^{-1}. The specific
153 sampling systems can be seen in Figure S2. Each sampling practice covered a whole
154 fuel-burning period. A total of 52 sets of samples were obtained.
155 For coal-fired power plants, 6 L summa cans were used to collect the flue gas
156 after diluted. Each sampling time lasted for about 23 hours. The power plant has
157 adopted ultra-low emission pollutant control measures, including wet desulfurization,
158 electric dust precipitation, and denitrification. Detailed information on the plant and
159 field sampling settings can be found in our former research (Zeng et al., 2021).
160 **2.2 CFC-11 analysis, quality assurance and quality control**
161 CFC-11 was analyzed by a gas chromatography/mass spectrometry (GC-MS,
162 Agilent 7820A/5977E). Samples were preconcentrated using a cold trap to remove
163 water and CO_2, with 300 mL of gas extracted from Tedlar bags or summa cans. The
164 concentrated analytes were then injected into a BD-624 chromatographic columns (60
165 m × 0.25 mm × 1.4 μm) via helium carrier gas. The GC system employed a dual-
166 detector configuration: effluent from the column was split between an FID and an MS
167 detector. The chromatographic column temperature was programmed from 35 ℃ to
168 180 ℃ at 6 ℃ min^{-1}. Both detectors were maintained at 200 ℃. The MS operated in
169 EI mode (70 eV) for ionization. An internal standard method was used to calculate the
170 concentration. Four internal standard substances including bromochloromethane, 1,4-
171 difluorobenzene, chlorobenzene, and 4-bromofluorobenzene are used. CFC-11 was
172 determined with a Mass Selective Detector (MSD) by the target ion at m/z 103/101,
173 and this method was widely used in previous research (Huang et al., 2021; Jin et al.,
174 2025; Zhang et al., 2014). GC-MS was also used in other research for CFC-11
175 observation (Park et al., 2021)
176 For quality control and quality assurance, tedlar bags were not reused in this
177 study. A system blank test was conducted, after every 10 samples were analyzed and

after the samples were analyzed at high concentrations. The calibration curves were updated monthly. A parallel sample was analyzed for every 10 samples or each batch (less than 10 samples), to ensure that the relative deviations of the targets were less than or equal to 30%. If the relative deviations exceeded 30%, then the sample was re-analyzed. Before each sample analysis, the air and water, the relative abundance of water, nitrogen, and oxygen should be less than 10%, otherwise the leakage of the instrument system should be checked. The detection limit of CFC-11 was 0.15 μg m^{-3}. The concentration of CFC-11 in the blank sample of the instrument is 0.

2.3 Calculation method of CFC-11 emission

The EFs of CFC-11 from domestic coal combustion were calculated as follows:

$$EF_i = \frac{(c_i \times \frac{v}{v_1} \times n - c_0) \times v_1 \times t \times 10^{-6}}{M_i} \quad (1)$$

Where *i* stood for the fuel type; *EFi* was the CFC-11 emission factor for combustion of fuel *i*, mg kg^{-1}; c_i was the mass concentration of CFC-11 in the sampling port after the combustion of fuel *i*, μg m^{-3}; *v* indicated the flow rate of flue gas, L min^{-1}; v_i indicated the sampling flow rate, L min^{-1}; *n* stood for dilution ratio; c_0 was the mass concentration of CFC-11 in the atmospheric environment, in this study was 0.6 μg m^{-3}; *t* was the sampling time, min; M_i was the weight of fuel *i* burned, kg. The average mass concentration of CFC-11 from domestic coal combustion was 93.9 ±90.4 μg m^{-3}, which was 150.7 times that of the ambient concentration, which indicated that the impact of ambient CFC-11 concentrations on its emission from coal combustion sources can be ignored.

The EFs of CFC-11 from coal-fired power plants were calculated as follows:

$$\mathrm{m_i} = \mathrm{c_i} \times \mathrm{v_1} \times \mathrm{t} \times 10^{-6} \quad (2)$$

$$\mathrm{EF_{ij}} = \frac{\mathrm{v} \times \mathrm{m_i} \times r_j^2 \times \mathrm{n}}{\mathrm{v_1} \times \mathrm{M_i} \times r^2} \quad (3)$$

Where *i* stood for the fuel type; m_i was the emission amount of CFC-11 released from the combustion of fuel *i*, mg; c_i was the mass concentration of CFC-11 from stack, which ignored the CFC-11 ambient concentration, μg m^{-3}; v_1 indicated the sampling flow rate, L min^{-1}; *t* was the sampling time, min; EF_{ij} was the CFC-11

emission factor emitted by the combustion of coal i from power plant j, mg kg^{-1}; r_j was the semidiameter of the stack at the sampling point, m; r was the semidiameter of the sampling nozzle, m; n stood for dilution ratio; v indicated the flow rate of flue gas, L min^{-1}; M_i was the weight of coal i burned, kg.

The CFC-11 emission amounts were calculated by multiplying its EFs (Table S2) with corresponding coal consumption amounts each year in China. The coal consumption amounts for each province of China from 2000~2021 were obtained from the China Energy Statistical Yearbook, and there were no data for Hong Kong, Macao, Taiwan, and Xizang (China energy statistical yearbook). The coal consumption amounts from 2022~2060 were calculated according to the decrease rate in references (Wu et al., 2024; Energy Foundation, 2024). The spatial distribution of CFC-11 from domestic coal combustion was allocated according to the 2000~2018 land use data with 30 m*30 m and 2000~2021 population distribution data with 1 km*1 km (WorldPop and Center for International Earth Science Information Network) (Gong et al., 2019, 2020). The land use data for 2019~2021 used the data in 2018. The Point of Interest (POI) data of industrial were obtained to allocate the CFC-11 emission from coal-fired power plants into each plant (Figure S3). The specific calculation and allocation method could be found in our former studies (Cheng et al., 2022; Wu et al., 2021).

When using CO as a tracer to calculate the CFC-11 emissions, the equation was adopted as follows (Palmer et al., 2003):

$$E_{CFC-11} = E_{CO} \times \frac{\Delta CFC-11}{\Delta CO} \times \frac{M_{CFC-11}}{M_{CO}} \quad (4)$$

Where E_{CFC-11} was the CFC-11 emissions, t; E_{CO} was the CO emissions, t; $\frac{\Delta CFC-11}{\Delta CO}$ was the slope of the linear correlation between ΔCFC-11 and ΔCO; M_{CFC-11} and M_{CO} were the molecular weights of CFC-11 and CO.

The CO_2-equivalent (CO_2-eq) emissions were calculated by multiplying the CFC-11 emission amounts with its global warming potential (GWP) value of 7090 (Burkholder et al., 2022).

2.4 WRF-FLEXPART modeling

Previous study identified Shandong and Hebei provinces as the dominant source regions for CFC-11 detected on islands near Korea and Japan (Park et al., 2021). Here, we tried to explore the influence of CFC-11 emissions from coal combustion in the two provinces on its ambient levels. FLEXPART was usually employed for inverse estimating CFC-11 emissions by former researchers (An et al., 2012; Park et al., 2021; Rigby et al., 2019). Here, January was heating period with higher coal combustion, and the year 2016 had higher CFC-11 emissions (Montzka et al., 2018), January 2016 was selected as the simulated period. The meteorological input data were obtained and downloaded from National Centers for Environmental Prediction (NCEP) Final Analysis (FNL; https://rda.ucar.edu/), which provided the lateral boundary conditions and initial meteorological fields for the simulation. The FNL data had a horizontal resolution of 1°× 1° and a temporal interval of 6 hours. The simulation domain encompassed the East Asian region (within the boundary of 20~47°N and 110~140°E). Hebei and Shandong were identified as the primary CFC-11 release areas. The simulation period was set for January 2016 (similar to the monitoring period in former studies) (Park et al., 2021), utilizing the forward modeling approach for analysis. Air parcels were released from the gridded emission areas over Hebei and Shandong provinces at altitudes from the surface up to 100 m, reflecting the near-ground emissions from coal combustion.

3. Results and discussion

3.1 CFC-11 EFs for coal combustion and comparison with other sources

The EFs of CFC-11 from chunk coal and honeycomb briquette combustion varied from 0.3~12.7 mg kg^{-1} (3.6±2.9 mg kg^{-1}) and 0.6~4.2 mg kg^{-1} (3.2±0.7 mg kg^{-1}), respectively (Figure 1). These values were 144 and 128 times higher than the EF for coal-fired power plant (0.025 mg kg^{-1}). The honeycomb briquette had higher combustion efficiency than chunk coal, which may reduce the release of chloride and formation of CFC-11 (Li et al., 2016). The much lower EFs for coal-fired power plant

could be related to the high combustion temperature and series of flue gas treatment measures (Yan et al., 2016). CFC-11 includes chloride (Cl) and fluoride (F), and the formation of CFC-11 needs the participation of them. F and Cl were widely distributed in coal (Jin et al., 2025; Yang et al., 2017). Former studies indicated that F content varied in 20~300 mg kg^{-1} from coals in the North China Plain and Northwest China, lower than those from the Southwest China (50~3000 mg kg^{-1}) (Luo et al., 2004). Yang et al. (2017) reported that the F content in China's coal varied in 11~3575 mg kg^{-1}, with an average value of 130 mg kg^{-1}. Chen et al. (2010) collected 305 kinds of coal samples all around China and analysis the Cl content, and indicated that the Cl content varied in 13.2~2815 μg g^{-1}. Jin et al. (2025) reported that the chlorine content of bituminous coal was 252.5 mg kg^{-1} in China. The formation and emission mechanisms of CFC-11 during coal combustion remained unclear. There was only one old literature reported that CFC-11 could be detected from the combustion of all tested 23 types of coal, and the release of CFC-11 peaked at a combustion temperature of 400 ℃ (Li et al., 2004). Coal combustion could emit halogenated organic compounds, such as methyl chloride (CH_3Cl) and chloroform (CH_2Cl_2) (Liu et al., 2024). Recent research presented the possible formation route of CFC-11 from above halogenated organic compounds in the iron and steel industry, based on the traditional liquid-phase fluorination method (Liu et al., 2024). This exploratory study primarily deduced that the formation conditions of CFC-11 in coal combustion were similar to the industrial synthesis conditions of CFC-11. The transformation pathways of solid fluoride in coal to CFC-11 and influencing parameters were still a puzzle. The mechanisms driving the formation and release of CFC-11, as well as the dominant influencing factors, remain unexplored and warrant further investigation.

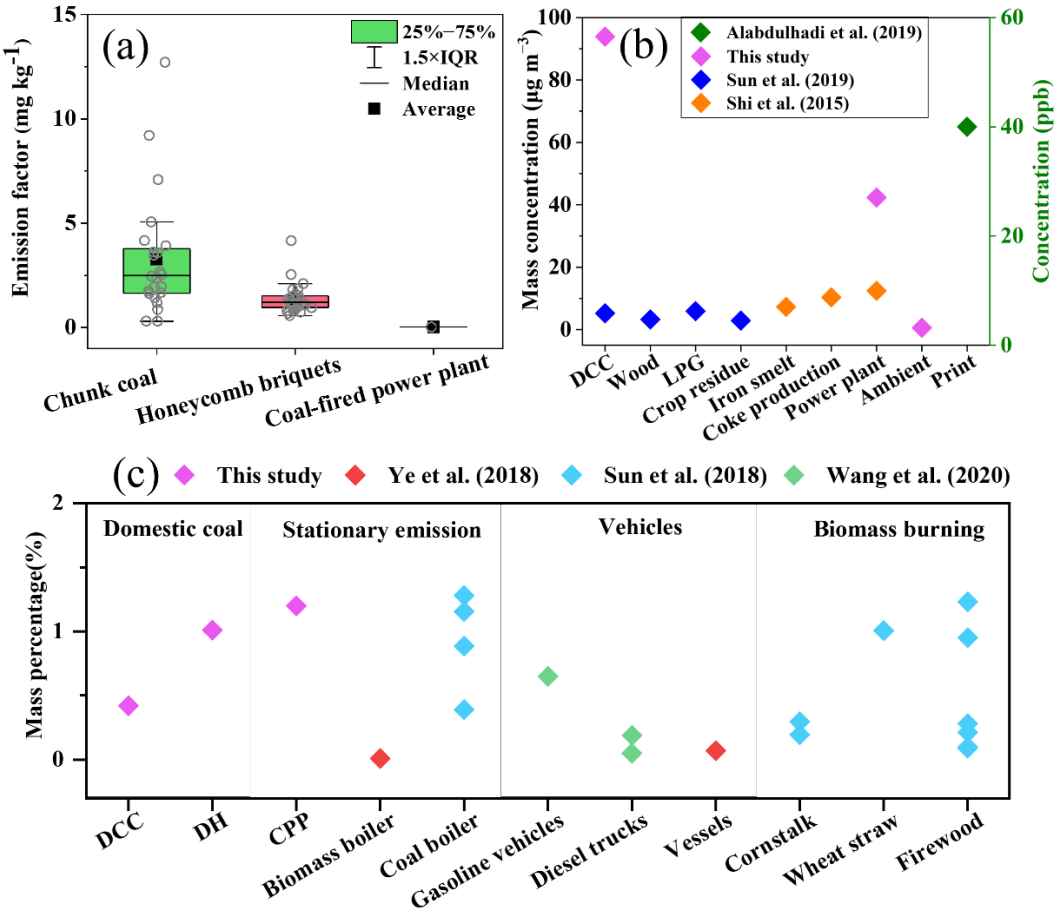

Figure 1. Comparison of CFC-11 emission from coal combustion and other sources for its emission factor (a), mass concentration (b), and mass percentage (c) in total VOCs. The VOCs included 102, 61, 107, 101, 98, and 102 species in this study, Sun et al. (2019), Shi et al. (2015), Ye et al. (2018), Sun et al. (2018), and Wang et al. (2020), respectively. DCC means domestic chunk coal, DH means domestic honeycomb, and CPP means coal-fired power plant.

Previous studies have reported the emission of CFC-11 from other anthropogenic sources (Gong et al., 2019; Sun et al., 2019). Domestic anthracite coal combustion (5.2 μg m^{-3}) (Sun et al., 2019), coating (44.5 μg m^{-3} and 91.0 μg m^{-3}), and printing (40 ppb and 10.9 μg m^{-3}) all emitted CFC-11 (Alabdulhadi et al., 2019; Shen et al., 2018). Figure 1b presented the CFC-11 mass concentration for reported combustion sources in the literature, coal-fired power plants (42.3 μg m^{-3}), iron smelting (7.3 μg m^{-3}), coke production (10.3 μg m^{-3}), and coal-fired power plants (12.5 μg m^{-3}) (Shi et al., 2015) all were the CFC-11 emission sources. The CFC-11 accounted for 0.4%, 1.0%, and 1.2% of the total volatile organic compounds (VOCs) detected from the

combustion of chunk coal, honeycomb briquette, and coal-fired power plant in this study, respectively. The CFC-11 also detected from stationary combustion of biomass (0.01%) (Ye, 2018), heavy-duty diesel trucks (0.05% or 0.2%) (Wang et al., 2020), vessels (0.07%) (Ye, 2018), and corn stover burning (0.3% or 0.2%) had also been reported in the literature (Figure 1c) (Sun et al., 2018). Ground measurement campaigns also recorded high CFC-11 levels from specific events, such as 626 ppt and 658 ppt for garbage burning and a landfill fire near Mecca, respectively (Simpson et al., 2022). Although combustion-related CFC-11 emissions were influenced by combustion conditions, these findings provided evidence for the contribution of coal combustion and other combustion sources to overall CFC-11 emissions.

3.2 Spatial-temporal distribution of CFC-11 from coal combustion in China

The annual CFC-11 emissions from coal combustion in China during 2000~2021 exhibited fluctuations and an overall upward trend, peaking at 268.7 t yr^{-1} in 2016 (Figures 2a–2b). CFC-11 emissions increased after 2012, consistent with previous studies that reported rising CFC-11 concentrations in ambient air (Adcock et al., 2020; Montzka et al., 2018; Rigby et al., 2019). Approximately 40%~60% of the global increase in CFC concentration was attributed to China, particularly Shandong and Hebei provinces (Adcock et al., 2020; Montzka et al., 2018; Rigby et al., 2019). This study found marked increases in CFC-11 emissions from Hebei (14.3 t yr^{-1}) and Shandong (11.0 t yr^{-1}) in 2013, which were 2.2 and 1.4 times the respective emission amounts in 2012 (Figure 3). The emission of CFC-11 emissions from coal combustion in China fluctuated during 2001~2021, averaging 233.5 t yr^{-1}. The contribution of coal combustion to CFC-11 emissions on a global scale needs further research.

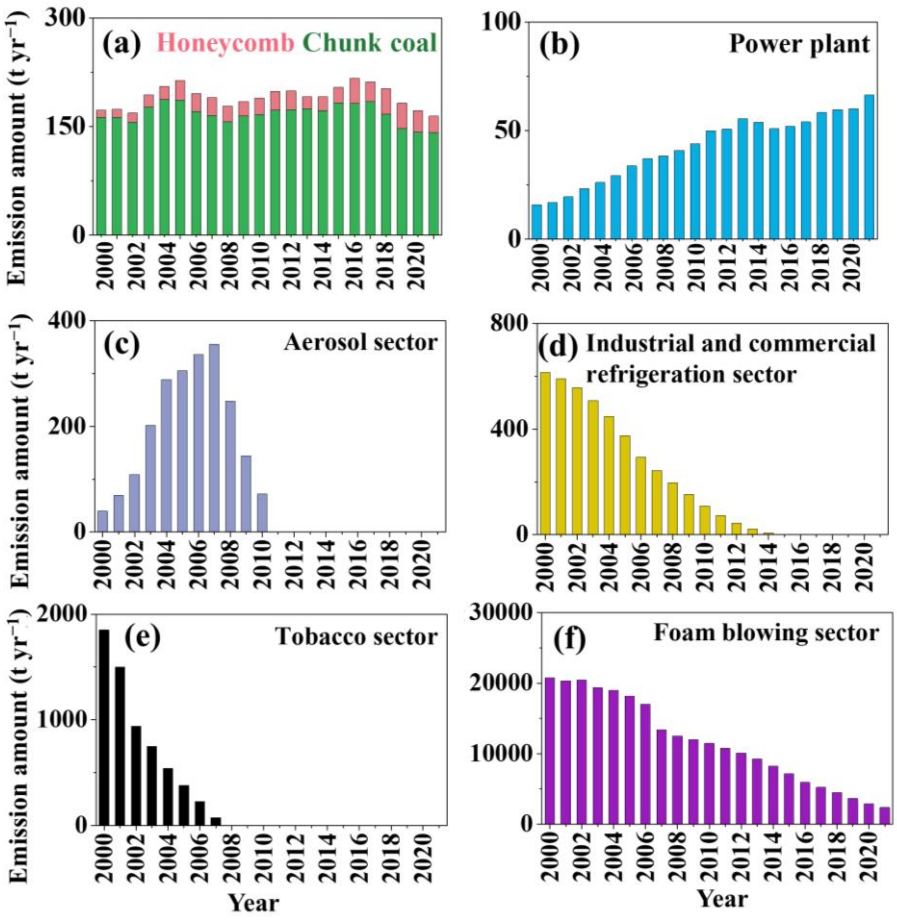

Figure 2. Annual CFC-11 emission from domestic coal combustion (a), coal-fired power plant (b), aerosol sectors (c), industrial and commercial refrigeration sector (d), tobacco sector (e), and foam blowing sector (f) in China. The data for (a) and (b) were calculated in this study. The data for (c)~(f) referred to Fang et al. (2018).

Although the contribution of domestic chunk coal combustion to CFC-11 annual emissions decreased from 2000 to 2021, it was still the dominant contributor, accounting for 60.9%~86.4% of CFC-11 emissions of domestic coal combustion in China (Figure 3). By 2021, the cumulative CFC-11 emissions from coal combustion reached 5135.7 t in China (Figure S4), with domestic coal combustion contributing 4200.0 t and coal-fired power plant contributing 935.7 t. With the transformation of China's energy structure, the proportion of CFC-11 emissions from coal-fired power plants in total CFC-11 emissions from coal combustion increased from 7.9% in 2000 to 18.2% in 2021.

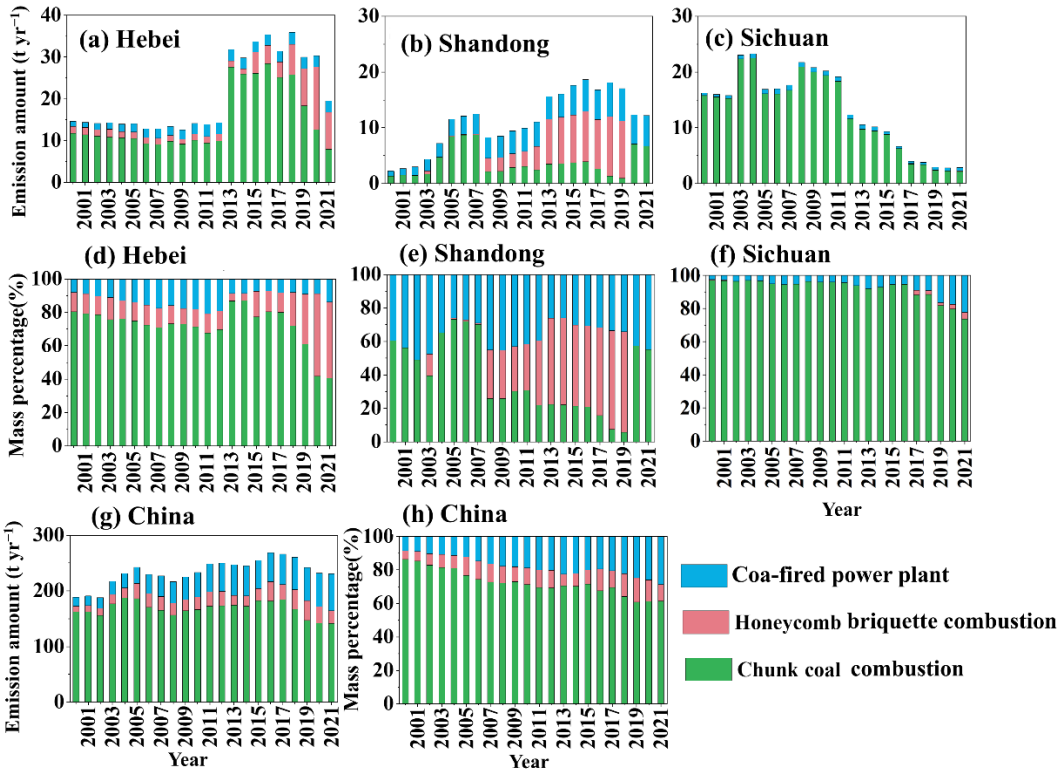

Figure 3. The CFC-11 emission amounts (a~c) and mass percentages (d~f) from power plant, domestic chunk coal, and honeycomb combustion in Hebei, Shandong, Sichuan provinces and China (g and h).

Previous studies have constructed CFC-11 emission inventories for its PAU processes and formed a PAU emission bank (Fang et al., 2018; Wan et al., 2009), which mainly included the sectors of aerosol, industrial and commercial refrigeration, tobacco, and foam-blowing in China as Figures 2c–2f shown. The CFC-11 emission amounts from coal combustion were comparable with those from aerosol sector and industrial and commercial refrigeration. The CFC-11 emissions from aerosol sector and tobacco sector disappeared after 2010 and 2007 as the Montreal Protocol, respectively. After 2015, the foam-blowing sector became the sole contributor to CFC-11 emissions among these sectors, with its emission declining to 7155.9 t yr^{-1}. If all other CFC-11 emissions from PAU sources were gradually getting to zero, while the CFC-11 emissions from coal combustion persisted, the influence of CFC-11 emissions from coal combustion should be considered at that time, especially when the CFC-11 emissions from PAU were cleared to zero.

Figure S5 presents the CFC-11 emissions from coal combustion in different provinces in China during 2000~2021. Provinces in heating areas (Figure S6) exhibited high CFC-11 emissions throughout the study period, they were in the north of China. Such as Inner Mongolia, Hebei, Henan, Xinjiang, Shandong, and Shanxi, the CFC-11 emissions in 2021 were 36.1 t, 19.5 t, 10.0 t, 21.2 t, 12.2 t, and 15.2 t respectively. Figure 4 and Figure S7 shows the CFC-11 emission intensity of CFC-11 from domestic coal combustion. High-emission areas were consistently concentrated in the North China Plain, including Hebei, Shandong, and Henan, where residential coal consumption has historically been significant. Over time, these high-emission zones became more pronounced, particularly after 2013.

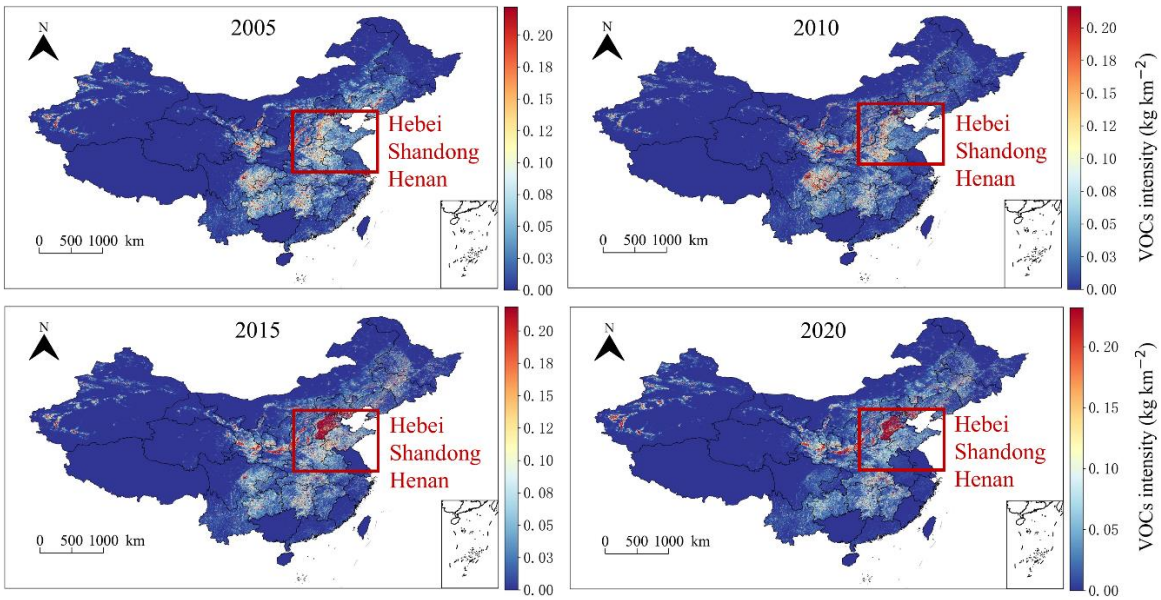

Figure 4. CFC-11 emission intensity of CFC-11 from domestic coal combustion in 2005, 2010, 2015, and 2020.

3.3 Comparison with CFC-11 emission obtained from CFC/CO ratios

In this study, the slope of CFC-11 and CO from coal combustion was 0.447 (Figure 5), higher than 0.039~0.087 in the atmosphere (Huang et al., 2021). CFC-11 emission inventory from coal combustion was obtained according to the CO emission inventory from coal combustion and CFC-11/CO ratio. Figure 5b presents the CFC-11 emission from coal combustion using CO tracer method and bottom-up method. The

CFC-11 emission through CO tracer method was 7872~60466 kt yr^{-1}, much higher than the emission using bottom-up method (7.9~60.8 t yr^{-1}). Although the ratio method using CO as a tracer was commonly applied in estimations, it might lead to an overestimation of CFC-11 emissions. Since CO had many emission sources, if the ratio was calculated using CFC-11/CO in the atmospheric concentration, then CFC-11 was also assumed to come from these emission sources. From previous research, CFC-11 emission from combustion sources, including industrial processes, vehicle emissions, garbage burning, LPG, and biomass burning, had long been overlooked (Shen et al., 2018; Wu & Xie, 2017; Zhang et al., 2020). However, the growing significance of these emissions highlighted the need for a more comprehensive evaluation of all potential sources for CFC-11, including above combustion sources and non-combustion sources like fuel oil storage, oil transportation, and printing facilities (Alabdulhadi et al., 2019b).

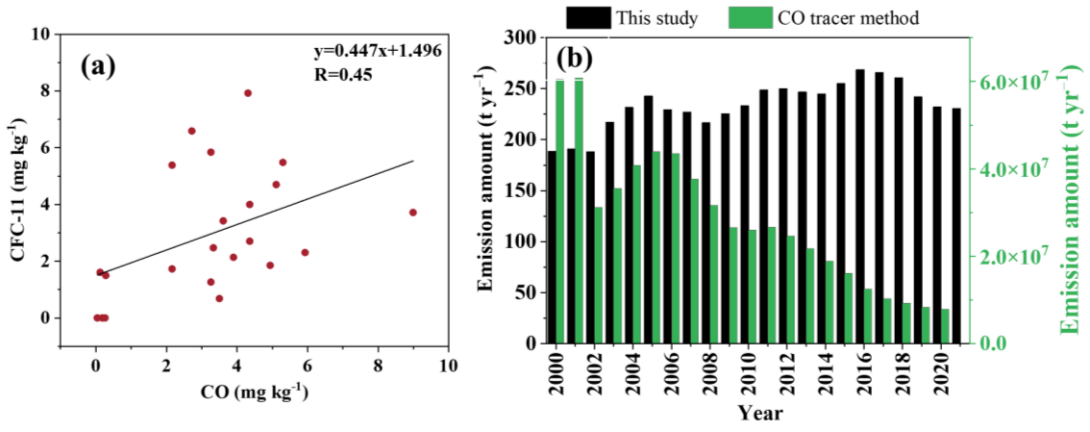

Figure 5. Interspecies correlations of CFC-11 with CO from coal combustion, R=Pearson's r (a), and comparison of CFC-11 emissions from coal combustion between this study and the CO tracer method. The emission inventory of CO for coal combustion was refereed to previous studies (b) (Liu et al., 2015; Peng et al., 2019; Tong et al., 2018).

3.4 Increasing importance of coal combustion in CFC-11 emission

A lot of research calculated the CFC-11 emissions in China and even globally based on ambient monitoring data (Table S3), the CFC-11 emissions from coal combustion were smaller than all CFC-11 emissions in China. The proportion of

CFC-11 emissions from coal combustion relative to its bank emissions increased year by year from 2000 (Figure 6a). The annual CFC-11 emissions from coal combustion in China from 2000 to 2021 varied from 188.5~268.7 t yr^{-1}, accounting for 1.5%~2.1% of the global increase in CFC-11 emission of 13±5 kt yr^{-1} reported in the literature (Montzka et al., 2018). In 2000, the CFC-11 emission from coal combustion was 188.5 t yr^{-1}, only accounting for 0.8% of PAU emissions in China. By 2021, however, CFC-11 emissions from coal combustion had risen to 9.8% of PAU emissions according to Figure 6a. After 2025, the CFC-11 emissions from PAU in China was 0 (Fang et al., 2018), but the CFC-11 from coal combustion still existed as seen in Figure S8, subsequent controls should give greater consideration to coal combustion because of its widespread sources (Jin et al., 2025).

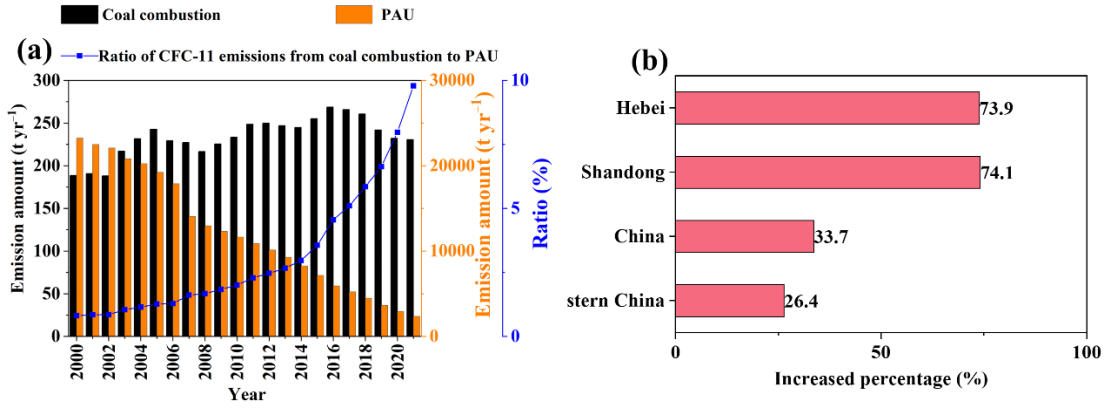

Figure 6. (a) Comparison of CFC-11 emission amounts from coal combustion (including coal consumed in domestic use and power plant) with CFC-11 emission from production and use (PAU) including aerosol sectors, tobacco sector, foam blowing sector, and industrial and commercial refrigeration sector in China (Fang et al., 2018). (b) The increased percentages for CFC-11 in this study in 2014~2017 compared to 2011~2012.

CFC-11 emissions from coal combustion increased sharply in 2013 as seen in Figure 2. From 2014 to 2017, CFC-11 emissions from coal combustion in China, Shandong Province, and Hebei Province increased compared to their corresponding emissions in the 2011~2012 period, the increasing ratios were 33.7%, 74.1%, and 73.9%, respectively (Figure 6b). Previous studies indicated that the concentration of CFC-11 in the northern hemisphere's atmosphere in 1995 was approximately 267 ppt

(Montzka et al., 2018). In 2060, the concentration of CFC-11 is 136.7 ppt, and in 2100, the concentration of CFC-11 still has 69.5 ppt (Daniel et al., 2022). Considering the lifetime of CFC-11 is about 52 years (Burkholder et al., 2022), we inferred that coal combustion might slightly contribute to the 136.7 ppt and 69.5 ppt of CFC-11.

3.5 Additional climate benefits of clean heating and coal-to-electricity policies

As the clean coal and heating policies were implemented, the coal consumption structures differed in southern (taking Sichuan as an example) and northern provinces (Hebei and Shandong) and changed quickly, which led to a clear variation of CFC-11 emission from coal combustion (Figure 3). The CFC-11 emission from honeycomb briquette combustion increased for Hebei and Shandong Province after 2013 when the Action Plan for Air Pollution Prevention and Control in China was released (Geng et al., 2024). In Sichuan province, CFC-11 emissions from chunk coal combustion decreased significantly, especially after 2013. By 2020, no CFC-11 emissions from honeycomb briquette combustion were detected in Shandong and Sichuan Province.

With the replacement of chunk coal with honeycomb briquette and coal-to-electricity policy, the emission of CFC-11 from chunk coal combustion gradually decreased after 2016 for China (Figure S9). Domestic coal combustion was projected to cease entirely by 2030 (Energy Foundation, 2024), and CFC-11 emissions from coal-fired power plant decreased gradually to zero in 2060 to realize carbon neutrality (Figure S9) (Wu et al., 2024). From 2000 to 2060, the cumulative CFC-11 emissions from coal combustion in China will be 7115.0 t. Even though the coal consumption structure had changed (Shen et al., 2022), coal combustion remained a stable emission source of CFC-11. Its accumulated emission amounts were similar to the historical (2000~2060) CFC-11 emissions from tobacco sector (6263 t), and higher than that of aerosol sector (4233 t) and industrial and commercial refrigeration (2169 t).

Figure 7 illustrates the CO_2-eq emissions in China from coal combustion between 2000 to 2021. In 2021, the CO_2-eq emissions reached 1.7×10^6 t yr^{-1}, accounting for 0.02% of total anthropogenic CO_2 emissions in China and 0.2% of CO_2

emissions from cement from Global Carbon Atlas. This value accounted for 0.03% of China's forest carbon sink (6.6×10^9 t CO_2) (Liu et al., 2015; Pan et al., 2011). These findings highlighted the need to reassess the role of CFC-11 from combustion emissions in global warming potential. From Figure 7b, the contribution of chunk coal combustion to CO_2-eq emissions decreased from 89.3% in 2000 to 63.3% in 2021 and would decrease to 0 after 2030. The replacement of chunk coal with honeycomb briquette resulted in a decrease of 25.2% in chunk coal usage and 8.9% in honeycomb usage (China Energy Statistical Yearbook). During 2000~2021, if all chunk coal was replaced by honeycomb briquette, CFC-11 and CO_2-eq emissions would be reduced by 10.6~16.0 t yr^{-1} and 7.5 $\times10^4$~1.1 $\times10^5$ t yr^{-1}, respectively (Figures S6 and 7c). This study verified the necessity of energy mix adjustment and the use of clean energy, from the aspect of co-prevention and control of multi-pollutants and the win-win in climate-environmental benefits (Shen et al., 2019; Shen et al., 2021; Tao et al., 2021). Although the decreased CFC-11 and CO_2-eq emissions were small, their impacts on the ozone layer and climate change should not be underestimated because of the extensive and universal sources of CFC-11 emissions (Jin et al., 2025).

In contrast, the contribution of coal-fired power plant to CO_2-eq emissions increased from 6.8% in 2000 to 28.0% in 2021 and was expected to rise to 100% after 2030. The coal-to-electricity strategy implemented in China increased the coal consumption in power plant (Wang et al., 2020), significantly reducing CFC-11 emissions from domestic coal combustion by 170.1~252.0 t yr^{-1} and reducing CO_2-eq emissions by 1.2×10^6~1.8×10^6 t yr^{-1} during 2000~2021 (Figures S6 and 5d). It indicates that transitioning to cleaner coal alternatives can not only improve the air quality in the North China Plain (Fang et al., 2019), but also yield unexpected significant climate benefits by reducing CFC-11 and CO_2-eq emissions. However, CFC-11 has a very large and uncertain indirect radiative cooling effect due to its depletion of Ozone, resulting in an indirect GWP of -4390 (Daniel et al., 2022). CO_2-eq emission in this study was calculated using direct GWP, relying solely on the direct

GWP might overestimate its climate impact. Therefore, a more comprehensive approach was essential for accurately assessing the full climate impact of CFC-11 and informing effective mitigation strategies.

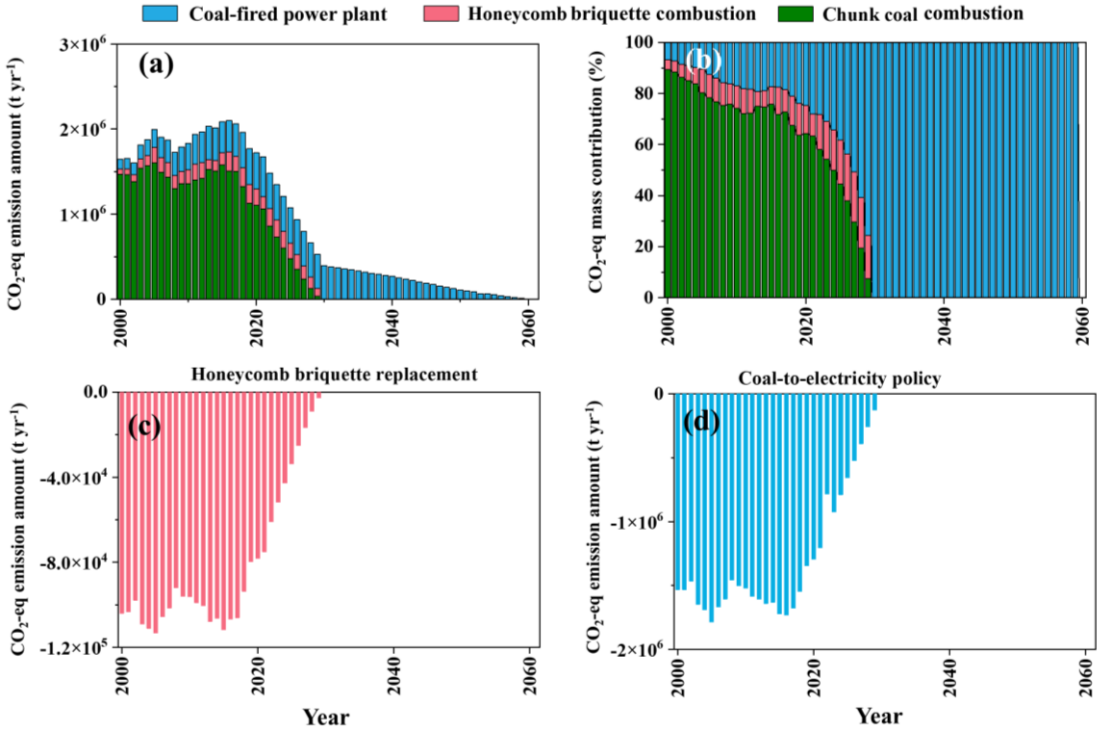

Figure 7. (a) Annual CO_2-eq emission amounts and (b) CO_2-eq mass contribution for CFC-11 emitted from coal combustion in China in this study. The changes of CO_2-eq emissions from CFC-11, if coal was replaced by honeycomb (c) and if domestic coal was replaced by electricity produced in coal-fired power plant (d).

3.6 The influence of CFC-11 from coal combustion on ambient concentration

Former researchers indicated that additional emission of CFC-11 was found in 2016 (Montzka et al., 2018; Rigby et al., 2019), monthly CFC-11 emission is presented in Figure 8. The monthly CFC-11 emissions from domestic coal combustion were allocated according to Wu et al. (2021), from coal-fired power plant were allocated according to the power generation volume from National Bureau of Statistics of China (https://www.stats.gov.cn/). The higher CFC-11 emissions from domestic coal combustion were in cold months, January (22.1 t), February (22.1 t), October (22.1 t), November (26.1 t), and December (24.1 t). The higher CFC-11 emissions from coal-fired power plant were in August (4.9 t) and December (5.0 t).

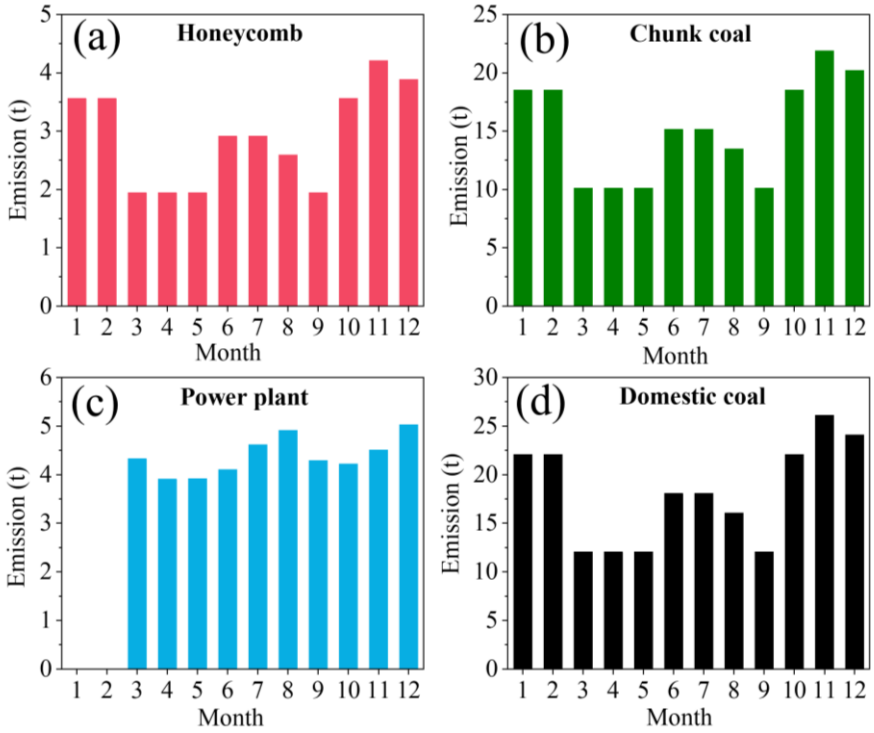

493

494 **Figure 8.** Monthly CFC-11 emissions from domestic honeycomb briquette combustion (a),
495 domestic chunk coal combustion (b), coal-fired power plant (c), and domestic coal combustion (d)
496 in 2016. The CFC-11 emissions from coal-fired power plant in January and February didn't have
497 specific data.

498 Shandong and Hebei Province were regarded as the hot source regions of CFC-
499 11 (Montzka et al., 2018; Rigby et al., 2019), from Figure 9a, Hebei and Shandong
500 provinces held high emission intensities of CFC-11 from coal combustion, with
501 average emission intensities of 0.23 kg km^{-2} and 0.03 kg km^{-2}, respectively. We also
502 found that the CFC-11 emission from coal combustion in Hebei and Shandong
503 provinces peaked in 2016 (Figures 9b–9c). They increased by 11.2% and 19.7%,
504 compared with those of 2013, then decreased by 15.2% and 8.6% in 2019,
505 respectively. Based on the WRF-FLEXPART modeling, we found that the CFC-11
506 emissions from coal combustion in Shandong and Hebei provinces could impact
507 South Korean areas (Figures 9d–9e). CFC-11 emissions from coal combustion in the
508 two provinces could lead to enhanced atmospheric concentrations of 254~1062 ppt
509 within a 410 km radius of the source regions during January. These values exceed the

observed CFC-11 concentration of 249 ± 13 ppt at Mount Tai during winter 2017~spring 2018 (Huang et al., 2021). The influence within 410 km is unlikely to extend to the monitoring stations outside China. Specifically, CFC-11 emissions from coal combustion in Hebei were simulated to contribute 51.8 ppt of the ambient CFC-11 at the Gosan station in South Korea. Similarly, the contributions from Shandong were simulated as 17.6 ppt. At the Gosan station in South Korea, the measured CFC-11 concentration was 233.2 ppt in January 2021 through the Advanced Global Atmospheric Gases Experiment (AGAGE, https://www-air.larc.nasa.gov/missions/agage/). Our simulations suggested that CFC-11 emissions from coal combustion in Hebei and Shandong contributed approximately 51.8 ppt and 17.6 ppt, respectively. They accounted for ~30% of the measured ambient value.

Although this suggested that regional coal combustion sources could slightly influence background monitoring data in coastal East Asia, the contribution remained much smaller than from global PAU-related emissions and must be interpreted cautiously. Notably, the results here also exhibited uncertainties or shortages. Firstly, the CFC-11 emission factors from chunk coal and honeycomb briquettes varied in a large range, with the ratios of maximum to minimum values as 42 and 7 times, and relative standard deviations of 61% and 81%, respectively. Secondly, the quick variation of domestic coal consumption amount and structure had not been reflected in the statistical yearbooks. The uncertainty of CFC-11 emission inventory from coal combustion in 2021 was ±50.2% through 100000 Monte Carlo simulations with a 95% coincidence interval. In this study, the coefficients of variation (CV, the standard deviation divided by the mean) for coal consumption amounts in power plant were assumed as 5%, and for domestic coal consumption it was set as 20% (Zhao et al., 2011). The uncertainty for EFs was referred to the standard deviation of it as given in Table S2.

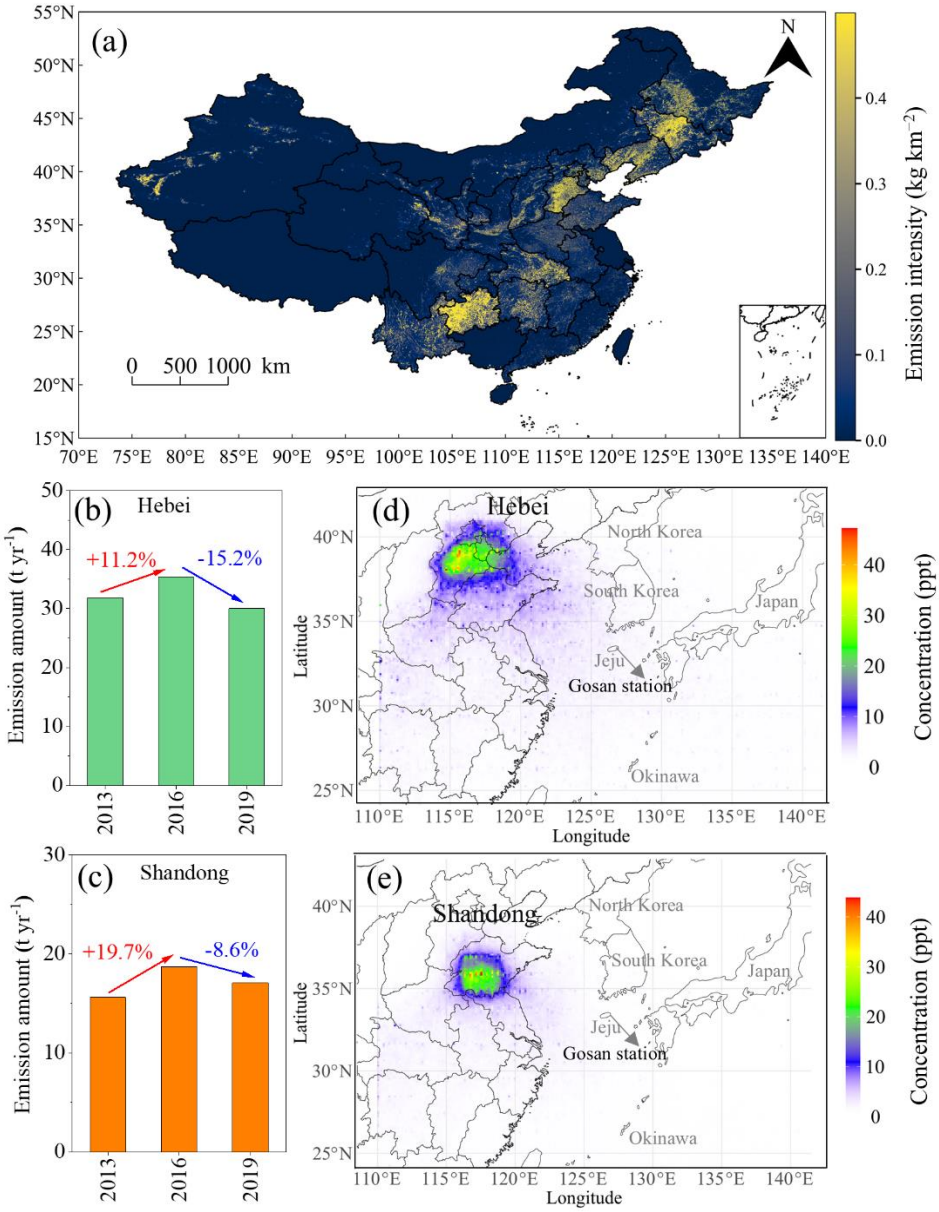

Figure 9. The emission intensity (kg km^{-2}) of CFC-11 from coal combustion in 2016 (a), and the changes of CFC-11 from coal combustion in 2013, 2016, and 2019 in Hebei province (b) and Shandong province (c) in China. The distribution of simulated CFC-11 mass concentration contributed by coal combustion in January 2016 from Hebei (d) and Shandong (e) provinces with WRF-FLEXPART.

4. Data availability

The dataset presented is available at https://doi.org/10.6084/m9.figshare.28523063 (Niu et al., 2025). The activity data of coal combustion were from the China Energy Statistical Yearbook. Land use data was from https://data-starcloud.pcl.ac.cn/ (Gong et al., 2019, 2020). Population

distribution data were from https://hub.worldpop.org/doi/10.5258/SOTON/WP00674 (WorldPop and Center for International Earth Science Information Network). The POI data of industrial were obtained from https://lbs.amap.com/. The CO emissions from coal combustion in China were from http://meicmodel.org.cn/#firstPage (Multiresolution Emission Inventory for China). The meteorological input data were obtained and downloaded from https://rda.ucar.edu/ (National Centers for Environmental Prediction Final Analysis).

5. Conclusions

There is currently no quantitative research on CFC-11 emissions from coal combustion. This study addresses that gap by estimating CFC-11 emissions in China from 2000 to 2021, based on coal consumption data and experimentally determined emission factors. The measured CFC-11 EFs were 3.6, 3.2, and 0.025 mg kg^{-1} from domestic chunk coal, honeycomb briquettes, and coal-fired power plants, respectively. During the study period, total CFC-11 emissions from coal combustion in China were estimated at 233.5 t yr^{-1}. In Shandong and Hebei provinces, which have high levels of coal consumption, CFC-11 emissions increased by approximately 74% during 2014~2017 compared to 2011~2012. At the Gosan monitoring station near mainland China, emissions from Hebei and Shandong accounted for approximately 30% of the average CFC-11 concentration in January 2016. Notably, China's clean heating and coal-to-electricity policies also brought climate co-benefits, resulting in significant reductions of CO_2-equivalent emissions by 2.2×10^6 t and 3.4×10^7 t, respectively. This study provides quantitative evidence of CFC-11 emissions from coal combustion, but the formation mechanisms of CFC-11 from coal combustion are unclear and need further investigation.

Author contributions:

ZN: Conceptualization, Experiments, Visualization, Writing; SK: Conceptualization, Methodology, Supervision, Writing-review & editing. QY, YC, HZ, and JW:

Experiments. YH, XQ, HD, and WJ: Visualization. YY, WL, FD, YB, and SQ: Supervision.

Competing interests:

The contact author has declared that none of the authors has any competing interests.

Financial Support:

This work was supported by the Key Technologies Research and Development Program (grant no. 2023YFC3709802), the Hubei Provincial Science Fund for Distinguished Young Scholars (grant no. 2022CFA040), and the National Natural Science Foundation of China (grant no. 42077202).

584 **References**

585 Adcock, K. E., Ashfold, M. J., Chou, C. C.-K., Gooch, L. J., Mohd Hanif, N., Laube,
586 J. C., et al. (2020). Investigation of East Asian emissions of CFC-11 using
587 atmospheric observations in Taiwan. *Environmental Science & Technology*, *54*(7),
588 3814–3822. https://doi.org/10.1021/acs.est.9b06433

589 Alabdulhadi, A., Ramadan, A., Devey, P., Boggess, M., & Guest, M. (2019).
590 Inhalation exposure to volatile organic compounds in the printing industry.
591 *Journal of the Air & Waste Management Association*, *69*(10), 1142–1169.
592 https://doi.org/10.1080/10962247.2019.1629355

593 An, X., Henne, S., Yao, B., Vollmer, M. K., Zhou, L., & Li, Y. (2012). Estimating
594 emissions of HCFC-22 and CFC-11 in China by atmospheric observations and
595 inverse modeling. *Science China Chemistry*, *55*(10), 2233–2241.
596 https://doi.org/10.1007/s11426-012-4624-8

597 Burkholder, J. B., Hodnebrog, Ø., McDonald, B. C., Orkin, V., Papadimitriou, V. C.,
598 & Van Hoomissen, D. (2022). Summary of abundances, lifetimes, ODPs, REs,
599 GWPs, and GTPs. World Meteorological Organization (WMO), Geneva,
600 Switzerland. https://csl.noaa.gov/assessments/ozone/2022/

601 Cheng, Y., Kong, S., Yao, L., Zheng, H., Wu, J., Yan, Q., et al. (2022). Multiyear
602 emissions of carbonaceous aerosols from cooking, fireworks, sacrificial incense,
603 joss paper burning, and barbecue as well as their key driving forces in China.
604 *Earth System Science Data*, *14*(10), 4757–4775. https://doi.org/10.5194/essd-14-
605 4757-2022

606 Chen, L. (2010). Study on environmental geochemistry of Chlorine in Chinese coals.
607 Nanchang University.

608 Chiodo, G., & Polvani, L. M. (2022). New insights on the radiative impacts of ozone-
609 depleting substances. *Geophysical Research Letters*, *49*(10), e2021GL096783.
610 https://doi.org/10.1029/2021GL096783

611 Daniel, J. S., Reimann, S., Ashford, P., Fleming, E. L., Hossaini, R., Lickley, M. J., et
612 al. (2022). 2022 Ozone Assessment, United Nations Environment Programme:
613 Nairobi, Kenya, 390–430. From chrome-
614 extension://efaidnbmnnnibpcajpcglclefindmkaj/https://csl.noaa.gov/assessments/
615 ozone/2022/downloads/Chapter7_2022OzoneAssessment.pdf
616 Dhomse, S. S., Feng, W., Montzka, S. A., Hossaini, R., Keeble, J., Pyle, J. A., et al.
617 (2019). Delay in recovery of the Antarctic ozone hole from unexpected CFC-11
618 emissions. *Nature Communications*, *10*(1), 5781. https://doi.org/10.1038/s41467-
619 019-13717-x
620 Fang, X., Ravishankara, A. R., Velders, G. J. M., Molina, M. J., Su, S., Zhang, J., et al.
621 (2018). Changes in emissions of ozone-depleting substances from China due to
622 implementation of the Montreal Protocol. *Environmental Science & Technology*,
623 *52*(19), 11359–11366. https://doi.org/10.1021/acs.est.8b01280
624 Fang, D., Chen, B., Hubacek, K., Ni, R., Chen, L., Feng, K., et al. (2019). Clean air
625 for some: unintended spillover effects of regional air pollution policies. *Science*
626 *Advances*, *5*(8), eaav4707. https://doi.org/10.1126/sciadv.aav4707
627 Fleming, E. L., Newman, P. A., Liang, Q., & Daniel, J. S. (2020). The impact of
628 continuing CFC-11 emissions on stratospheric ozone. *Journal of Geophysical*
629 *Research: Atmospheres*, *125*(3), e2019JD031849.
630 https://doi.org/10.1029/2019JD031849
631 Geng, G., Liu, Y., Liu, Y., Liu, S., Cheng, J., Yan, L., et al. (2024). Efficacy of China's
632 clean air actions to tackle $PM_{2.5}$ pollution between 2013 and 2020. *Nature*
633 *Geoscience*, *17*, 987–994. https://doi.org/10.1038/s41561-024-01540-z
634 Global Carbon Atlas. Carbon Emissions. Available at:
635 https://globalcarbonatlas.org/emissions/carbon-emissions/ (accessed December
636 22, 2024).

637 Gong, P., Chen, B., Li, X., Liu, H.,Wang, J., Bai, Y., et al. (2020). Mapping essential
638 urban land use categories in China (EULUCChina): Preliminary results for 2018,
639 *Science Bulletin*, *65*, 182–187. https://doi.org/10.1016/j.scib.2019.12.007
640 Gong, P., Li, X., & Zhang, W. (2019). 40-Year (1978–2017) human settlement
641 changes in China reflected by impervious surfaces from satellite remote sensing,
642 *Science Bulletin*, *64*(11), 756–763. https://doi.org/10.1016/j.scib.2019.04.024
643 Guo, H., Ding, A., Wang, T., Simpson, I. J., Blake, D. R., Barletta, B., et al. (2009).
644 Source origins, modeled profiles, and apportionments of halogenated
645 hydrocarbons in the greater Pearl River Delta region, Southern China. *Journal of*
646 *Geophysical Research: Atmospheres*, *114*(D11), 2008JD011448.
647 https://doi.org/10.1029/2008JD011448
648 Huang, X., Zhang, Y., Xue, L., Tang, J., Song, W., Blake, D. R., & Wang, X. (2021).
649 Constraining emission estimates of CFC-11 in Eastern China based on local
650 observations at surface stations and Mount Tai. *Environmental Science &*
651 *Technology Letters*, *8*(11), 940–946. https://doi.org/10.1021/acs.estlett.1c00539
652 Jin, W., Yan, Y., Qiu, X., Peng, L., Li, Z., & Tang, Y. (2025). Characterizing full-phase
653 chlorine species emissions from domestic coal combustion in China:
654 Implications for significant impacts on air pollution and ozone-layer depletion.
655 *Environmental Pollution*, 372, 126043.
656 https://doi.org/10.1016/j.envpol.2025.126043
657 Kim, J., Li, S., Kim, K., Stohl, A., Mühle, J., Kim, S., et al. (2010). Regional
658 atmospheric emissions determined from measurements at Jeju Island, Korea:
659 Halogenated compounds from China. *Geophysical Research Letters*, *37*(12),
660 2010GL043263. https://doi.org/10.1029/2010GL043263
661 Li, J., Wang, J., Li, H., Rao, Z., Li, Q., & Luo, S. (2003). The production and release
662 of CFCs from coal combustion. *Acta Geologica Sinica-English Edition*, *77*(1),
663 81–85. https://doi.org/10.1111/j.1755-6724.2003.tb00113.x

Li, J., Wang, J., Yao, Z., Li, H., Li, Q., Luo, S., et al. (2004). Production and Emission of Chlorofluorocarbons during Coal Combustion. *Rock and Mineral Analysis*, *23* (1), 1–5. (In Chinese) https://doi.org/10.15898/j.cnki.11-2131/td.2004.01.001

Lickley, M., Fletcher, S., Rigby, M., & Solomon, S. (2021). Joint inference of CFC lifetimes and banks suggests previously unidentified emissions. *Nature Communications*, *12*(1), 2920. https://doi.org/10.1038/s41467-021-23229-2

Liu, F., Zhang, Q., Tong, D., Zheng, B., Li, M., Huo, H., et al. (2015). High-resolution inventory of technologies, activities, and emissions of coal-fired power plants in China from 1990 to 2010, *Atmospheric Chemistry and Physics*, *15*, 13299–13317. https://doi.org/10.5194/acp-15-13299-2015

Liu, Y., Weng, W., Zhang, Q., Li, Q., Xu, J., Zheng, L., et al. (2024). Ozone-depleting substances unintendedly emitted from iron and steel industry: CFCs, HCFCs, halons and halogenated very short-lived substances. *Journal of Geophysical Research: Atmospheres*, *129*(17), e2024JD041035. https://doi.org/10.1029/2024JD041035

Liu, Z., Guan, D., Wei, W., Davis, S. J., Ciais, P., Bai, J., et al. (2015). Reduced carbon emission estimates from fossil fuel combustion and cement production in China. *Nature*, *524*(7565), 335–338. https://doi.org/10.1038/nature14677

Luo, K., Ren, D., Xu, L., Dai, S., Cao, D., Feng, F., & Tan, J. (2004). Fluorine content and distribution pattern in Chinese coals. *International Journal of Coal Geology*, *57*(2), 143–149. https://doi.org/10.1016/j.coal.2003.10.003

McCulloch, A., Ashford, P., & Midgley, P. M. (2001). Historic emissions of fluorotrichloromethane (CFC-11) based on a market survey. *Atmospheric Environment*, *35*(26), 4387–4397. https://doi.org/10.1016/S1352-2310(01)00249-7

689 Molina, M. J., & Rowland, F. S. (1974). Stratospheric sink for chlorofluoromethanes:
690 chlorine atom-catalysed destruction of ozone. *Nature*, *249*(5460), 810–812.
691 https://doi.org/10.1038/249810a0
692 Montzka, S. A., Dutton, G. S., Yu, P., Ray, E., Portmann, R. W., Daniel, J. S., et al.
693 (2018). An unexpected and persistent increase in global emissions of ozone-
694 depleting CFC-11. *Nature*, *557*(7705), 413–417. https://doi.org/10.1038/s41586-
695 018-0106-2
696 Montzka, S. A., Dutton, G. S., Portmann, R. W., Chipperfield, M. P., Davis, S., Feng,
697 W., et al. (2021). A decline in global CFC-11 emissions during 2018−2019.
698 *Nature*, *590*(7846), 428–432. https://doi.org/10.1038/s41586-021-03260-5
699 National Bureau of Statistics of China, 2000–2021. China energy statistical yearbook
700 2001–2022. China Statistics Press, Beijing. From
701 http://cnki.nbsti.net/CSYDMirror/Trade/yearbook/single/N2022060061?z=Z024
702 Niu, Z., Kong, S., Yan, Q., Cheng, Y., Zheng, H., Hu, Y., et al. (2025). Estimation of
703 CFC-11 emissions from coal combustion in China, Figshare [data set],
704 https://doi.org/10.6084/m9.figshare.28523063.
705 Palmer, P. I., Jacob, D. J., Mickley, L. J., Blake, D. R., Sachse, G. W., Fuelberg, H. E.,
706 et al. (2003). Eastern Asian emissions of anthropogenic halocarbons deduced
707 from aircraft concentration data. *Journal of Geophysical Research: Atmospheres*,
708 *108*(D24), 2003JD003591. https://doi.org/10.1029/2003JD003591
709 Pan, Y., Birdsey, R. A., Fang, J., Houghton, R., Kauppi, P. E., Kurz, W. A., et al.
710 (2011). A large and persistent carbon sink in the world's forests. *Science*,
711 *333*(6045), 988–993. https://doi.org/10.1126/science.1201609
712 Park, S., Western, L. M., Saito, T., Redington, A. L., Henne, S., Fang, X., et al. (2021).
713 A decline in emissions of CFC-11 and related chemicals from eastern China.
714 *Nature*, *590*(7846), 433–437. https://doi.org/10.1038/s41586-021-03277-w
715 Peng, L., Zhang, Q., Yao, Z., Mauzerall, D. L., Kang, S., Du, Z., et al. (2019).
716 Underreported coal in statistics: A survey-based solid fuel consumption and

emission inventory for the rural residential sector in China, *Applied Energy*, *235*, 1169–1182. https://doi.org/j.apenergy.2018.11.043

Polvani, L. M., Previdi, M., England, M. R., Chiodo, G., & Smith, K. L. (2020). Substantial twentieth-century Arctic warming caused by ozone-depleting substances. *Nature Climate Change*, *10*(2), 130–133. https://doi.org/10.1038/s41558-019-0677-4

Pons, J., Tope, H., Walter-Terrinoni, H. (2019). Montreal protocol on substances that deplete the ozone layer, report of the technology and economic assessment panel May 2019, Volume 3: Decision XXX/3 TEAP Task Force Report on Unexpected Emissions of Trichlorofluoromethane (CFC-11). United Nations Environment Programme: Nairobi, Kenya. From https://ozone.unep.org/science/assessment/teap

Rigby, M., Prinn, R. G., O'Doherty, S., Montzka, S. A., McCulloch, A., Harth, C. M., et al. (2013). Re-evaluation of the lifetimes of the major CFCs and CH_3CCl_3 using atmospheric trends. *Atmospheric Chemistry and Physics*, *13*(5), 2691–2702. https://doi.org/10.5194/acp-13-2691-2013

Rigby, M., Park, S., Saito, T., Western, L. M., Redington, A. L., Fang, X., et al. (2019). Increase in CFC-11 emissions from eastern China based on atmospheric observations. *Nature*, *569*(7757), 546–550. https://doi.org/10.1038/s41586-019-1193-4

Scientific assessment of ozone depletion: 2018. (2019). Geneva, Switzerland: World Meteorological Organization. From https://csl.noaa.gov/assessments/ozone/2018/

Shao, M., Huang, D., Gu, D., Lu, S., Chang, C., & Wang, J. (2011). Estimate of anthropogenic halocarbon emission based on measured ratio relative to CO in the Pearl River Delta region, China. *Atmospheric Chemistry and Physics*, *11*(10), 5011–5025. https://doi.org/10.5194/acp-11-5011-2011

Shen, G., Ru, M., Du, W., Zhu, X., Zhong, Q., Chen, Y., et al. (2019). Impacts of air pollutants from rural Chinese households under the rapid residential energy

transition. *Nature Communications*, *10*(1), 3405. https://doi.org/10.1038/s41467-019-11453-w

Shen, G., Xiong, R., Tian, Y., Luo, Z., Jiangtulu, B., Du, W., et al. (2022). Substantial transition to clean household energy mix in rural households in China. *National Science Review*, *9*(7), nwac050. https://doi.org/10.1093/nsr/nwac050

Shen, H., Luo, Z., Xiong, R., Liu, X., Zhang, L., Li, Y., et al. (2021). A critical review of pollutant emission factors from fuel combustion in home stoves. *Environment International*, *157*, 106841. https://doi.org/10.1016/j.envint.2021.106841

Shen, L., Xiang, P., Liang, S., Chen, W., Wang, M., Lu, S., et al. (2018). Sources profiles of volatile organic compounds (VOCs) measured in a typical industrial process in Wuhan, Central China. *Atmosphere*, *9*(8), 297. https://doi.org/10.3390/atmos9080297

Shi, J., Deng, H., Bai, Z., Kong, S., Wang, X., Hao, J., et al. (2015). Emission and profile characteristic of volatile organic compounds emitted from coke production, iron smelt, heating station and power plant in Liaoning Province, China. *Science of The Total Environment*, *515–516*, 101–108. https://doi.org/10.1016/j.scitotenv.2015.02.034

Simpson, I. J., Barletta, B., Meinardi, S., Aburizaiza, O. S., DeCarlo, P. F., Farrukh, M. A., et al. (2022). CFC-11 measurements in China, Nepal, Pakistan, Saudi Arabia and South Korea (1998–2018): Urban, landfill fire and garbage burning sources. *Environmental Chemistry*, *18*(8), 370–392. https://doi.org/10.1071/EN21139

Sun, J., Shen, Z., Huang, Y., Cao, J., Ho, S. S. H., Niu, X., et al. (2018). VOCs emission profiles from rural cooking and heating in Guanzhong Plain, China and its potential effect on regional O_3 and SOA formation. *Atmospheric Chemistry and Physics Discussion.* https://doi.org/10.5194/acp-2018-36

Sun, J., Shen, Z., Zhang, L., Zhang, Y., Zhang, T., Lei, Y., et al. (2019). Volatile organic compounds emissions from traditional and clean domestic heating appliances in Guanzhong Plain, China: Emission factors, source profiles, and

effects on regional air quality. *Environment International*, *133*, 105252. https://doi.org/10.1016/j.envint.2019.105252

Tao, S., Shen, G., Cheng, H., & Ma, J. (2021). Toward clean residential energy: challenges and priorities in research. *Environmental Science & Technology*, *55*(20), 13602–13613. https://doi.org/10.1021/acs.est.1c02283

Tong, D., Zhang, Q., Liu, F., Geng, G., Zheng, Y., Xue, T., et al. (2018). Current emissions and future mitigation pathways of coal-fired power plants in China from 2010 to 2030, *Environmental Science & Technology*, *52*(21), 12905–12914. https://doi.org/10.1021/acs.est.8b02919, 2018

Tsinghua University Building Energy Efficiency Research Center, Energy foundation. (2024). Constructing a new rural energy system toward carbon nutrality-comprehensive report on the governance of rural domestic coal in China. Tsinghua University: Beijing, China (In Chinese). From https://www.ccetp.cn/newsinfo/7604069.html

Wan, D., Xu, J., Zhang, J., Tong, X., & Hu, J. (2009). Historical and projected emissions of major halocarbons in China. *Atmospheric Environment*, *43*(36), 5822–5829. https://doi.org/10.1016/j.atmosenv.2009.07.052

Wang, M., Li, S., Zhu, R., Zhang, R., Zu, L., Wang, Y., & Bao, X. (2020). On-road tailpipe emission characteristics and ozone formation potentials of VOCs from gasoline, diesel and liquefied petroleum gas fueled vehicles. *Atmospheric Environment*, *223*, 117294. https://doi.org/10.1016/j.atmosenv

Wang, M., Li, S., Zhu, R., Zhang, R., Zu, L., Wang, Y., et al. (2020). On-road tailpipe emission characteristics and ozone formation potentials of VOCs from gasoline, diesel and liquefied petroleum gas fueled vehicles. *Atmospheric Environment*, *223*, 117294. https://doi.org/10.1016/j.atmosenv.2020.117294

Wang, S., Su, H., Chen, C., Tao, W., Streets, D. G., Lu, Z., et al. (2020). Natural gas shortages during the “coal-to-gas” transition in China have caused a large

redistribution of air pollution. *Proceedings of the National Academy of Sciences*, *117*(49), 31018–31025. https://doi.org/10.1073/pnas.2007513117

Western, L. M., Vollmer, M. K., Krummel, P. B., Adcock, K. E., Crotwell, M., Fraser, P. J., et al. (2023). Global increase of ozone-depleting chlorofluorocarbons from 2010 to 2020. *Nature Geoscience*, *16*(4), 309–313. https://doi.org/10.1038/s41561-023-01147-w

Wu, H., Liu, J., Hu, X., He, G., Zhou, Y., Wang, X., et al. (2024). Fewer than 15% of coal power plant workers in China can easily shift to green jobs by 2060. *One Earth*, *7*(11), 1994–2007. https://doi.org/10.1016/j.oneear.2024.10.006

Wu, J., Kong, S., Zeng, X., Cheng, Y., Yan, Q., Zheng, H., et al. (2021). First high-resolution emission inventory of levoglucosan for biomass burning and non-biomass burning sources in China. *Environmental Science & Technology*, *55*(3), 1497–1507. https://doi.org/10.1021/acs.est.0c06675

Wu, R., & Xie, S. (2017). Spatial distribution of ozone formation in China derived from emissions of speciated volatile organic compounds. *Environmental Science & Technology*, *51*(5), 2574–2583. https://doi.org/10.1021/acs.est.6b03634

Yan, Q., Kong, S., Yan, Y., Liu, H., Wang, W., Chen, K., et al. (2020). Emission and simulation of primary fine and submicron particles and water-soluble ions from domestic coal combustion in China. *Atmospheric Environment*, *224*, 117308. https://doi.org/10.1016/j.atmosenv.2020.117308

Yan, Q., Kong, S., Yan, Y., Liu, X., Zheng, S., Qin, S., et al. (2022). Emission and spatialized health risks for trace elements from domestic coal burning in China. *Environment International*, *158*, 107001. https://doi.org/10.1016/j.envint.2021.107001

Yan, Y., Yang, C., Peng, L., Li, R., & Bai, H. (2016). Emission characteristics of volatile organic compounds from coal-, coal gangue-, and biomass-fired power plants in China. *Atmospheric Environment*, *143*, 261–269. https://doi.org/10.1016/j.atmosenv.2016.08.052

Yang, N., Tang, S., Zhang, S., Huang, W., Chen, P., Chen, Y., et al. (2017). Fluorine in Chinese coal: A review of distribution, abundance, modes of occurrence, genetic factors and environmental effects. *Minerals*, *7*, 219. https://doi.org/10.3390/min7110219

Ye, X. (2018). Study on characteristics of pollutants emission from non-road mobile source and biomass boilers on real work conditions. South China University of Technology.

Zeng, L., Dang, J., Guo, H., Lyu, X., Simpson, I. J., Meinardi, S., et al. (2020). Long-term temporal variations and source changes of halocarbons in the Greater Pearl River Delta region, China. *Atmospheric Environment*, *234*, 117550. https://doi.org/10.1016/j.atmosenv.2020.117550

Zeng, X., Kong, S., Zhang, Q., Ren, H., Liu, J., Feng, Y., et al. (2021). Source profiles and emission factors of organic and inorganic species in fine particles emitted from the ultra-low emission power plant and typical industries. *Science of The Total Environment*, *789*, 147966. https://doi.org/10.1016/j.scitotenv.2021.147966

Zhang, Y., Li, C., Yan, Q., Han, S., Zhao, Q., Yang, L., et al. (2020). Typical industrial sector-based volatile organic compounds source profiles and ozone formation potentials in Zhengzhou, China. *Atmospheric Pollution Research*, *11*(5), 841–850. https://doi.org/10.1016/j.apr.2020.01.012

Zhao, Y., Nielsen, C. P., Lei, Y., McElroy, M. B., and Hao, J. (2011). Quantifying the uncertainties of a bottom-up emission inventory of anthropogenic atmospheric pollutants in China. *Atmospheric Chemistry and Physics*, *11*, 2295–2308. https://doi.org/10.5194/acp-11-2295-2011